Int J Adv Manuf Technol (2017) 93:2227–2242
DOI 10.1007/s00170-017-0693-3

ORIGINAL ARTICLE

Tool overlap effect on redistributed residual stress and shape distortion produced by the machining of thin-walled aluminum parts

Xiaohui Jiang[1] · Zhenya Zhang[1] · Zishan Ding[1] · Omar Fergani[2] · Steven Y. Liang[3]

Received: 31 March 2017 / Accepted: 14 June 2017 / Published online: 29 June 2017

Abstract As the main factor, residual stress undoubtedly restricts the long-term stability of high-precision machining quality parts, arresting an extensive attention on studying its control method. Therefore, a model is meticulously proposed, along with the optimization method of the overlap rate of cutting tool path. In the roughing, the selection of a larger magnitude of overlap coefficient K is found to be necessary for the optimization of the surface machined residual stress, followed by an indispensable selection of smaller K values in the finishing. The shrinking overlap coefficient K echoes with the decreasing influence of the deformation affected by the residual stress distribution, inevitably accompanied by the lowering material removal rate. Based on all the optimization results, an aerospace thin-walled part is adopted in the application case to verify the proposed approach.

Keywords Tool overlap · Residual stress · Distortion · Milling · Thin-walled parts

✉ Xiaohui Jiang
jiangxh@usst.edu.cn

[1] College of Mechanical Engineering, University of Shanghai for Science & Technology, Yangpu, Shanghai, People's Republic of China

[2] NTNU-Department of Engineering Design and Material, Norwegian University of Science and Technology, Trondheim, Norway

[3] The George W. Woodruff School of Mechanical Engineering, Georgia Institute of Technology, Atlanta, GA, USA

1 Introduction

Being one of the main factors responsible for the quality of the key parts, the distribution of machined residual stress (RS) has been noticeably restricting and affecting the development of aerospace, automobile, shipbuilding, and other fields. Meanwhile, the continuous development of the new technology such as additive manufacturing has already posed a huge challenge to the traditional machining.

The focuses of recent researches have been gradually shifted to the generation of residual stress during the single machining procedure. Early in the 1952, Boiten and cate [1] proposed a method to measure the residual stresses in plates through the experiments on different processing parameters. Researchers have never ceased to work on the optimization of the processing and tool parameters in the past decades in order to achieve the ideal machined residual stress. Segawa et al. [2] developed a new tool that could generate compressive residual stress within the machined surface concurrently with the milling process. After that, Arunachalam et al. [3] suggested that the round CBN cutting inserts should be used at slow cutting speeds (150 m/min) and small depths of cut (0.05 mm) with the use of coolant, allowing the possibility of achieving the compressive or minimal tensile residual stresses and good surface finish. Navas et al. [4] studied the effect on the final surface stress state in AISI 4340 steel of cutting speed, feed, tool nose radius, geometry of the tool chip breaker, and coating of the cutting tool, harvesting the conclusion that the generation of surface tensile residual stresses depended on the cutting conditions and the characteristics of the cutting tool.

The very first effort in the redistribution of the residual stress was supposed to be contributed by Sasahara et al. [5] who got down to the first attempt to examine the effects of sequential cuts on RS, where such effects were meticulously

learnt (experimentally and numerically) with orthogonal cutting brass. The succeeding study carried out by Liu and Guo [6] analyzed the regenerated residual stress in the sequential cut process, and offered the finding that the possibility existed for the machined surface residual stress being transformed from tensile stress to compressive stress if only the second cutting process was optimized rationally. Nasr [7] dived into the effects of sequential cuts on residual stresses when orthogonal cutting steel AISI 1045, after which the initial stress state at the beginning of cutting was concluded as the main reason for ending up with different RS distribution after the second cut (compared to a stress-free state for the first cut). Beyond that, the redistribution of residual stress and distortion in machining was further explored by Wang et al. [8] via the removal of material layer-by-layer for a selected frame part with the material removal thickness of each layer varying from 2 to 3 mm. It was also elaborated by Outeiro et al. [9] that the model of finite element analysis (FEA), considering its effect on the increase of superficial residual stresses during the sequential cuts [10], should be further optimized so that it could better match the experimental processing. Robinson et al. [11] discussed the mechanisms of redistribution of machined residual stress for Al 7449 after heat treatment as well as the effect of the redistribution of the residual stress on the part distortion after the removal of the material layer by layer. However, no signs were observed on the stress release, and the model was limited to the rule cube object. At present, the research on the redistribution of residual stress had been conducted during the grinding [12] and micro-end-milling [13].

In brief, the scopes of all these studies are mainly fixed on the thickness of each layer (equal or nearly equal) of machined workpiece material, and the analysis of redistribution of the machined surface residual stress is limited to the machining of thin-walled part where different depths of cut are usually utilized [14]. Therefore, more influential factors are quite necessary to be taken into account for further analysis of the redistribution of residual stress, with an expectation for decreasing or maintaining the distortion of the thin-walled part.

Based on the existing results, the attentions of more researchers have been shifted to the residual stress and distortion of the parts, with some insightful conclusions being reached worldwide. For instance, Treuting and Read [15] first established a relationship between the stress and the curvature by removing the sheet material by multiple layers, which laid the foundation for the analysis of the redistribution of residual stress and distortion. After that, Sosa et al. [16] found that the mean stress of the residual stress profile in the tensile area indicated correlation with distortion, being greater for the highest nodule count samples. The under-addressed residual stress relaxations led to the occurrence of the deformations. According to Fergani et al. [17], a new methodology was proposed based on analytical modeling of machining mechanics to predict thin plate deflection induced by residual stresses. Moreover, being capable of predicting forces and residual stress distortion, another analytical model was introduced by Fergani et al. [18] for micromachining applications. In addition, Sasahara [19] put forward a longer fatigue life for the machined components, which could be realized through the application of the cutting conditions of a low feed rate, a small corner radius, and a chamfered cutting-edge tool.

As described above, the control method for residual stress and deformation still remains unclear since the existing research has not clarified the generation mechanism of redistribution of residual stress, and the relations are still ill-defined between the redistribution trends of residual stress and deformation changes of workpiece. Therefore, the exact relationship between the part distortions and redistribution of residual stress relaxations still awaits to be identified and analyzed scientifically, especially for the aerospace machining application. Here, a note is made, usually the redistribution of residual stress can be consisted by the surface and subsurface of parts. In the previous work [20], the effect of depth of cut on the subsurface residual stress regeneration is discussed. And an approach is proposed to optimize the residual stress of thin-walled parts. Therefore, in this study, the redistribution surface residual stress is analyzed with overlap coefficient K.

2 Methodology

2.1 Experimental procedure

As presented in the Fig. 1, the high-speed milling experiments were conducted by the five-axis machining center (Deckel MAHO DMU60P). With the chemical composition and main material properties of Al 2024-T3 machined for the experiments listed in the Table 1, the following analysis has revealed the directions of cutting forces in this paper being the tangential force (Ft), radial force (Fr), force in feed (Fy), and vertical directions (Fx), as indicated in Fig. 2. The processing and tool parameters are presented in Table 2.

The measuring method of the residual stress usually includes the drilling method (damage the workpiece), strain gauge, X-ray, and other technologies. Considering the high machining expense of thin-walled parts, the X-ray method is widely acknowledged as a better option that not only saves the measuring time but also avoids breaking the workpiece. Moreover, the material of target part is aluminum ally, which is more easy to be measured with

Fig. 1 Machining experiment

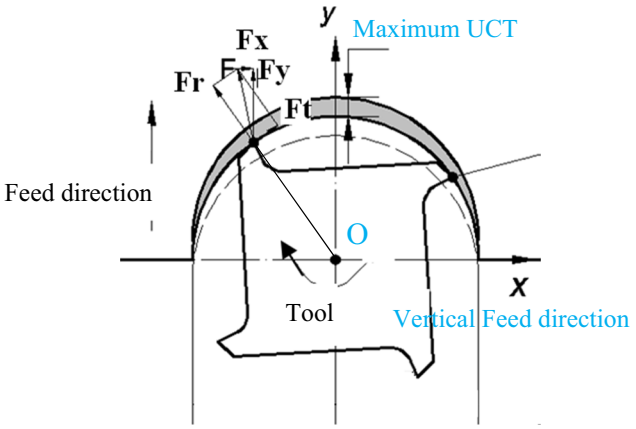

Fig. 2 Directions of cutting forces

X-ray approach. And the measurement error can be kept within ± 10 MPa under the appropriate settings of the stress analyzer. Therefore, the measurement results can be trusted and compared in the discussion part. In this study, after the milling machining experiments, the residual stress analyzer (LXRD Canada proto Fig. 3) is utilized to measure the machined residual stress of the workpiece under different technical parameters in the following discussion sessions. Moreover, the measurement scheme of the surface and subsurface residual stresses is shown in Fig. 4. Considering the maximum and minimum thickness of part is 8 and 2 mm, respectively; therefore, in the basic experiments, the part is designed accordingly in Fig.4. The parameter setup of the residual stress analyzer is manifested in Table 3.

2.2 Simulation procedure

The FE simulation technology is widely adopted by the researchers for calculating and predicting the residual stress while in this paper, the commercial software Third wave AdvantEdge™ is applied for the same purpose. It should be admitted that the material model (flow stress, material properties et al.) plays a vital role in the formation of cutting force, temperature and residual stress, and in fact, plenty of material models are used in the FEM, such as Johnson-Cook, Power Law, and Bodner-Partom et al. The prediction characteristics of these different material models were one compared by Jing and Liu [21]. In this study, as shown in Eq. (1), the model Power law is selected, with the flow stress curve (Al2024-T3) being defined in the material library of AdvantEdge™.

$$\sigma\left(\varepsilon^{p},\dot{\varepsilon},T\right)=g(\varepsilon^{p})\cdot\Gamma\left(\dot{\varepsilon}\right)\cdot\Theta(T) \tag{1}$$

where $g(\varepsilon^{p})$ is strain hardening, $\Gamma(\dot{\varepsilon})$ is strain rate sensitivity, and $\Theta(T)$ is thermal softening. While the strain hardening function g (ε^{p}) Eq. (2) for the power law is defined as:

$$\begin{aligned} g(\varepsilon^{p})&=\sigma_0\left(1+\frac{\varepsilon^{p}}{\varepsilon_0{}^{p}}\right)^{1/n}, if\ \varepsilon^{p}<\varepsilon_{cut}{}^{p},\\ g(\varepsilon^{p})&=\sigma_0\left(1+\frac{\varepsilon_{cut}{}^{p}}{\varepsilon_0{}^{p}}\right)^{1/n}, if\ \varepsilon^{p}\geq\varepsilon_{cut}{}^{p}, \end{aligned} \tag{2}$$

where σ_0 is the initial yield stress, ε^{p} is the plastic strain, $\varepsilon_0{}^{p}$ is the reference plastic strain, $\varepsilon_{cut}{}^{p}$ is the cutoff strain, and n is the strain hardening exponent. And the thermal softening function Θ (T) Eq. (3)for the power law is defined as:

$$\begin{aligned} \Theta(T)&=c_0+c_1T+c_2T^2+c_3T^3+c_4T^4+c_5T^5, if\ \ T<T_{cut}\\ \Theta(T)&=\Theta(T_{cut})\left(1-\frac{T-T_{cut}}{T_{melt}-T_{cut}}\right), if\ \ T\geq T_{cut} \end{aligned} \tag{3}$$

Where c_0 through c_5 are coefficients for the polynomial fit, T is the temperature, T_{cut} is the linear cutoff temperature, and T_{melt} the melting temperature.

Table 1 The chemical composition (%) and main mechanical properties of Al2024-T3

Chemical composition	Al	Cu	Mg	Mn	Mechanical properties	Tensile stress (MPa)	Yield stress (MPa)	Young's modulus (GPa)	Density (kg/m^3)	Poisson's ratio
	93.5	4.4	1.5	0.6		427	276	73	2780	0.3

Table 2 The processing and tool parameter setup for the analysis of the tool overlap experiments

Processing parameters	Feed rate *fz* [mm/tooth]	Depth of cut *ap* [mm]		Cutting width *ae* [mm]	Rotational speed *n* [rev/min]
	0.2	1		6~12	16,000
Tool parameters	Orthogonal rake angle [°]	Orthogonal clearance angle[°]	Helix angle [°]	Tool diameter [mm]	Material
	15	6	30	12	Carbide-grade

For the simulation model setup, the triangular elements are utilized for the mesh of tool and workpiece where the mesh size fall into the range between 0.16 and 0.01 mm. Smaller mesh size results in better results and more time to calculate; in this study, different mesh sizes have been tried in order to avoid the convergence error and obtain ideal results. In the Third Wave Systems can be found the definition and setup of the other parameters of the friction coefficient (0.5) (Bil et al., [22]) and heat transfer (Third Wave Systems [23]).

Figure 5a, b has exhibited the establishment of the AdvantEdge-3D milling model and the definition of the mesh model, respectively. In the feed direction, the removal of the material is accompanied by the redistribution of the stress as the tool rotates and feeds along with the workpiece. Attempting to predict the redistribution of residual stress under the multiple feed rate, better residual stress prediction abilities of the 3D modeling with the selected software, which in fact, are supported by many analysis cases (Marusich and Ortiz [24]; Marusich and Askari [25]) showing the effectiveness of the AdvantEdge-3D in predicting the cutting force, temperature, and residual stress.

2.3 Modeling procedure

Since different cutting processing, such as multiple cuts, will generate the redistribution of residual stress on the surface and subsurface of the workpiece, the processing parameters in different cutting times keep being adjusted to locate a method for optimizing the residual stress distribution. Hitherto, the completed and ongoing study (Treuting and Read [15], Liu and Guo [6]) in most researches has been still limited to constructing second cutting with inadequate research and discussion diving into the subsequent cuts that is considered to somehow constrain the analysis of multiple cuts on the redistribution of residual stress for machining of thin-walled parts. Therefore, in this study, the processing conditions are being changed without neglecting the residual stress distribution data measured by test and simulation, which allows the import of the residual stress profile into the finite element software to calculate the regenerated stress.

The removal of materials by the tool rotation results in breaking the equilibration of initial residual stress (Fig. 6a). Therefore, the residual stress within the material needs to be

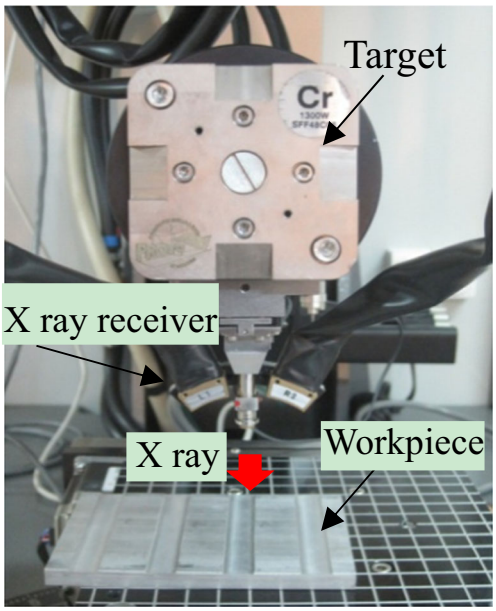

Fig. 3 Measurement of residual stress

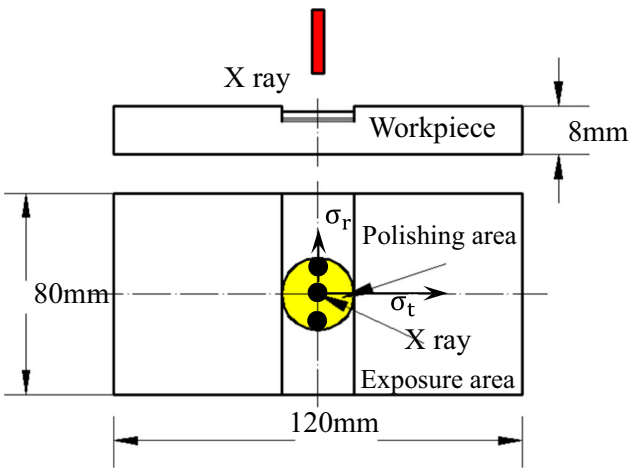

Fig. 4 Scheme of residual stress measurement

Table 3 X-ray diffraction parameters for residual stress measurement

Target	Aperture	Voltage	Elastic constant K	Bragg 2θ	Diffracting plane hkl	Ψ(±20°)	Oscillation beta angle
Cr	1 mm	25KV	−98.6124	156.31°	222	11	3°

redistributed for the balance again, inducing the distortion of the workpiece generated as shown in Fig. 6b. The sum area of A and C is equal to the area of B. When the material containing the stress C is cut, then the distortion occurs to balance the stress of A and B. Multiple depths of cut find its necessity in the milling of thin-walled part. In addition, it should note that the overlap of tool has influence on the surface and subsurface residual stress. The shape distortion of machined thin-walled part is determined by different passes milling, and will induce the distortion changes as in Fig.6b. The curvature relation of the workpiece before and after machining with the depth of cut (a_p), can be expressed as the following Eq. (4), along with the sequential deformation generated in the following processes:

$$\frac{1}{R_{\mathrm{n}}}-\frac{1}{R_{n-1}}=\frac{6a_pT_n\sigma_j}{E(T_{n-1})^3} \tag{4}$$

where n is the number of the layer; R_n and R_{n-1} are the curvature radius before and after the "n"th layer is stripped; T_n and T_{n-1} are the thickness of workpiece before and after the "n"th layer for each depth of cut is removed; σ_j is the stress before the "n"th layer is cut; E is the elastic modulus.

3 Results and discussions

Firstly, this section is composed of three parts to analyze the redistribution law of the residual stress, and the influence of redistribution on the deformation of the workpiece, with an expectation for an optimization method of the distribution state of residual stress. In order to obtain a proper residual stress state in the process of redistribution, the workpiece deformation caused by different distribution of residual stress in constant changes has been analyzed in the material removal process, with the theoretical basis being verified through the case study, whose results will be discussed in the Section 3.3.

3.1 Assessment of the redistribution surface residual stress in the feed and cutting direction

3.1.1 Analysis of the simulated and experimental redistribution of surface residual stress

In this section, experimental and simulated methods are first introduced to study the influence of the surface machined residual stress affected by the tool path overlap on the surface residual stress redistribution, for obtaining the optimization method of controlling the residual stresses.

As the experimental program shown in Fig. 7, the setup of processing parameters are presented in Table 4. The experimental and simulated results are accepted to test the redistribution of residual stress in the feed and the vertical feed direction during the milling process.

1) Comparison of redistribution of residual stress in the feed direction:

It can be observed in Table 5 that the cutting width is the tool diameter, and the removed material of the left half arc is from less to more, while the right half arc is from more to less. For groups 1 and 2, the removed material in the cutting

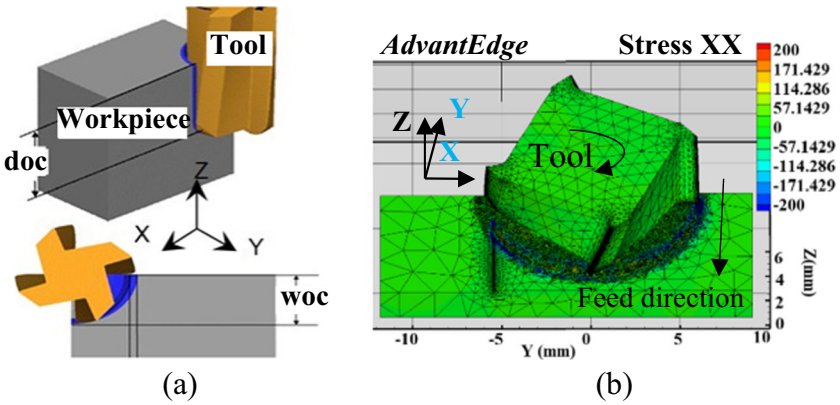

Fig. 5 **a** Milling model (Third Wave Systems, 2010). **b** Mesh and residual stress contour

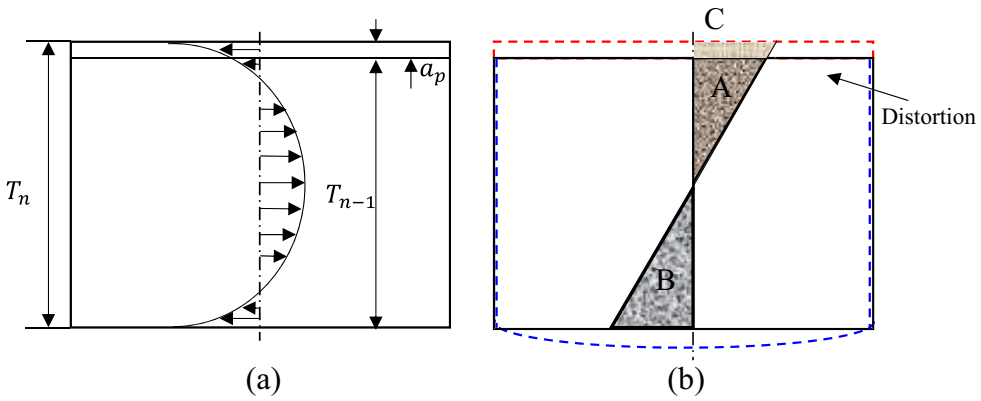

Fig. 6 **a** Initial residual stress distribution. **b** distortion induced by the redistribution of residual stress

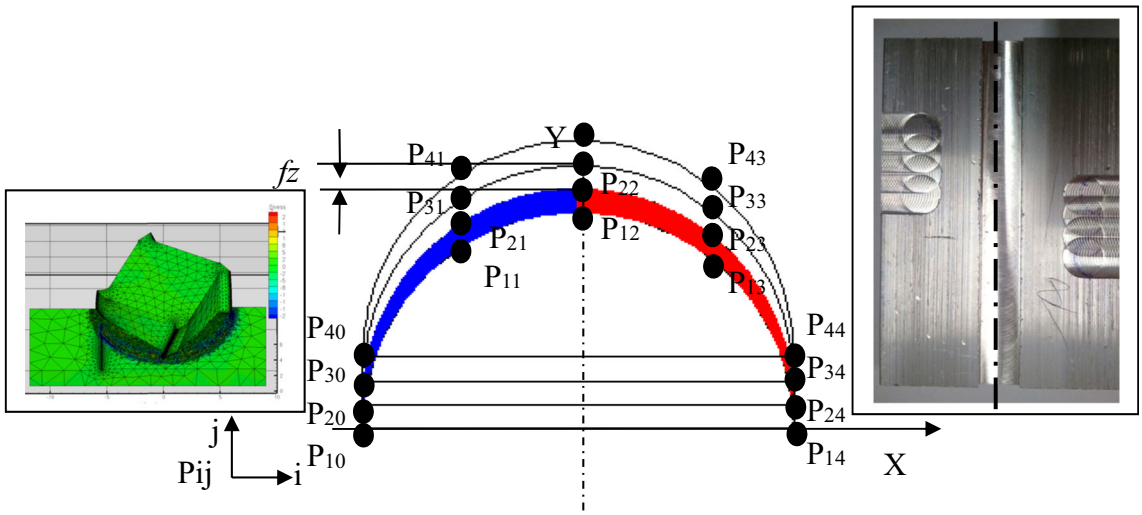

Fig. 7 The program of tool path overlap and analysis points in the feed directions

process is found to be squeezed by the rotated tool on both sides, resulting in the formation of residual compressive stresses (points P_{i0} and P_{i4}), and residual tensile stress in the middle of the tool path (points P_{i1}, P_{i2}, and P_{i3}). With the tool machining in the feed direction and through the comparison between the residual stress distribution in the four cutting laps, the finding is obvious that in the same direction, the changes of magnitude of residual stress for different points remain unnoticeable (No. 1 to No. 4), the rationale behind which lies in that the feed rate is a constant value in the feed direction, determining the value of the uncut chip thickness to stay the same and igniting the superimposition on the generated residual stress value varying a little. Moreover, as presented in Table 5, in order to average the uncertain resources, five exacting times around the marked points conducted to calculate the final residual stress. In addition, it was observed that the tested and predicted values were well matched. To a certain extent, the built methods can be used for further analysis and discussion.

2) Comparison of the redistribution of residual stress in the vertical feed direction:

After a large volume of material of thin-walled parts is removed, apart from the impact of the processing parameters, the superimposition between the tool cutting paths surely plays an important role in the redistribution of surface machined residual stress. Therefore, in this section, the focus is laid on the analysis of the influences of the superimposition area between tool paths. The cutting experimental parameters are given in the Table 2.

Table 4 Processing parameter setup for analysis of redistribution of residual stress in the feed direction

Group number	Rotational spindle speed *n* (rev/min)	Feed rate *fz* (mm/t)	Cutting width *ae* (mm)	Depth of cut *ap* (mm)
1	4000	0.2	12	0.1
2	18,000	0.2	12	0.1

Table 5 The average value of residual stress at different points

Cutting speed (rev/min)	P_{i0} (MPa)			P_{i1} (MPa)				P_{i2} (MPa)				P_{i3} (MPa)				P_{i4} (MPa)					
4000	NO.	X-FE	X-EXP	Y-FE	Y-EXP	X-FE	X-EXP	Y-FE	Y-EXP	X-FE	X-EXP	Y-FE	Y-EXP	X-FE	X-EXP	Y-FE	Y-EXP	X-FE	X-EXP	Y-FE	Y-EXP
	1	3	6	−6	−4	48	56	97	106	169	187	95	101	83	85	53	64	−21	−35	−4	−8
	2	1	8	−1	−2	79	81	221	197	140	165	129	136	108	114	104	112	−43	−50	−5	−10
	3	2	7	5	−1	79	83	123	153	122	116	150	164	118	125	144	154	−96	−83	−34	−38
	4	4	10	−4	3	98	103	181	199	187	198	196	189	132	145	136	163	−83	−89	−42	−48
Mean value		3	8	−2	−1	76	81	156	164	155	167	143	148	110	117	109	123	−61	−64	−21	−26
18,000	1	8	10	−11	−13	73	82	68	78	78	82	88	97	69	79	95	107	−35	−45	−19	−26
	2	13	16	−17	−23	61	75	38	56	76	86	178	181	119	139	154	167	−69	−56	−28	−32
	3	20	15	−27	−32	69	73	58	72	78	93	131	151	99	146	147	225	−18	−43	−14	−19
	4	25	32	−29	−36	71	85	182	186	104	117	191	206	285	243	335	298	−24	−31	−13	−16
Mean value		17	18	−21	−26	69	79	87	98	84	95	147	159	143	152	183	199	−37	−44	−19	−23

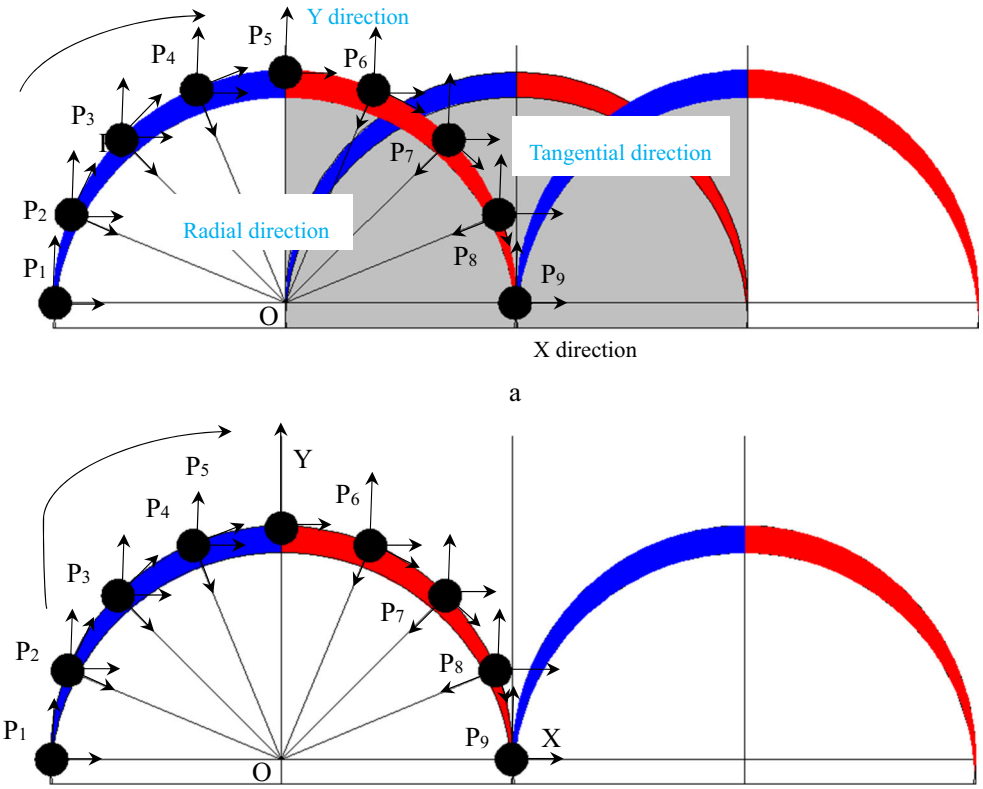

Fig. 8 **a** No.1 tool path (up- and down-milling with overlap). **b** No.2 tool path (up-milling without overlap)

As the two schemes presented in Fig. 8, No.1 tool path is machined with half of the diameter as the cutting width, while the diameter is used as the cutting width in the No.2 tool path. And, the residual stress is measured according to the points P1~P9 marked in Fig. 8. The residual stress is measured based on the four directions, which are the residual stress in X direction, Y direction, radial direction, and tangential direction. In this study, the up-milling and down-milling are both conducted in the comparison of the redistribution of the residual stress between the tool paths. The results are given in the Fig. 9.

Very similar to the discussion on the feed direction, the four-direction measurement of the residual stress in Fig. 10 has provided the information that the residual stress measured in the radial direction points P1 to P9 is actually not uniform, with the residual compressive stress being easily formed on both sides while the residue tensile stress tending to be formed in the middle of the cutting tool path. Through comparing the average value of horizontal line for residual stress in each direction of the same track, it can be disclosed that, for the three tested cutting methods, the minimum average value of the surface residual stress is obtained through up milling (No.1 tool path), while the maximum average value of the residual stress is reaped through the full tool diameter cutting without overlap (No.2 tool path). It has been also indicated that in the transverse cutting, the surface residual stress of the workpiece can be improved to a certain extent via the superposition of two adjacent tool cuttings, undoubtedly benefiting the improvement of the workpiece' quality. However, a contradictory problem arises that, when the tool does not stack cutting, the material removal rate will fall accordingly, requiring further exploration for the optimization relation between the material removal rate and the residual stress. The discussion about this would be organized in the following section.

3.1.2 Analysis of optimizing the machined redistribution of surface residual stress

Typically, multiple cuts are implemented for the milling of thin-walled parts where the milling tool path is of a certain overlap width, commonly known as the tool overlap coefficient. The calculation formula is expressed as Eq. (5). The tool overlap coefficient is mainly related to the diameter of the milling cutter, milling width, and the width of the cutting tool. The smaller the overlap coefficient, the greater width of transverse cutting tool, and vice versa, as shown in the Fig. 10, where Y is the feed direction, X direction of cutting width; the three circles are the rotation path of tool; the shaded part is the overlapping region of the milling cutter. The superposition effect is controlled to be varied for the investigation into the influence of overlap coefficient on the residual stress of the machined surface.

$$K = (D - ae)/D \tag{5}$$

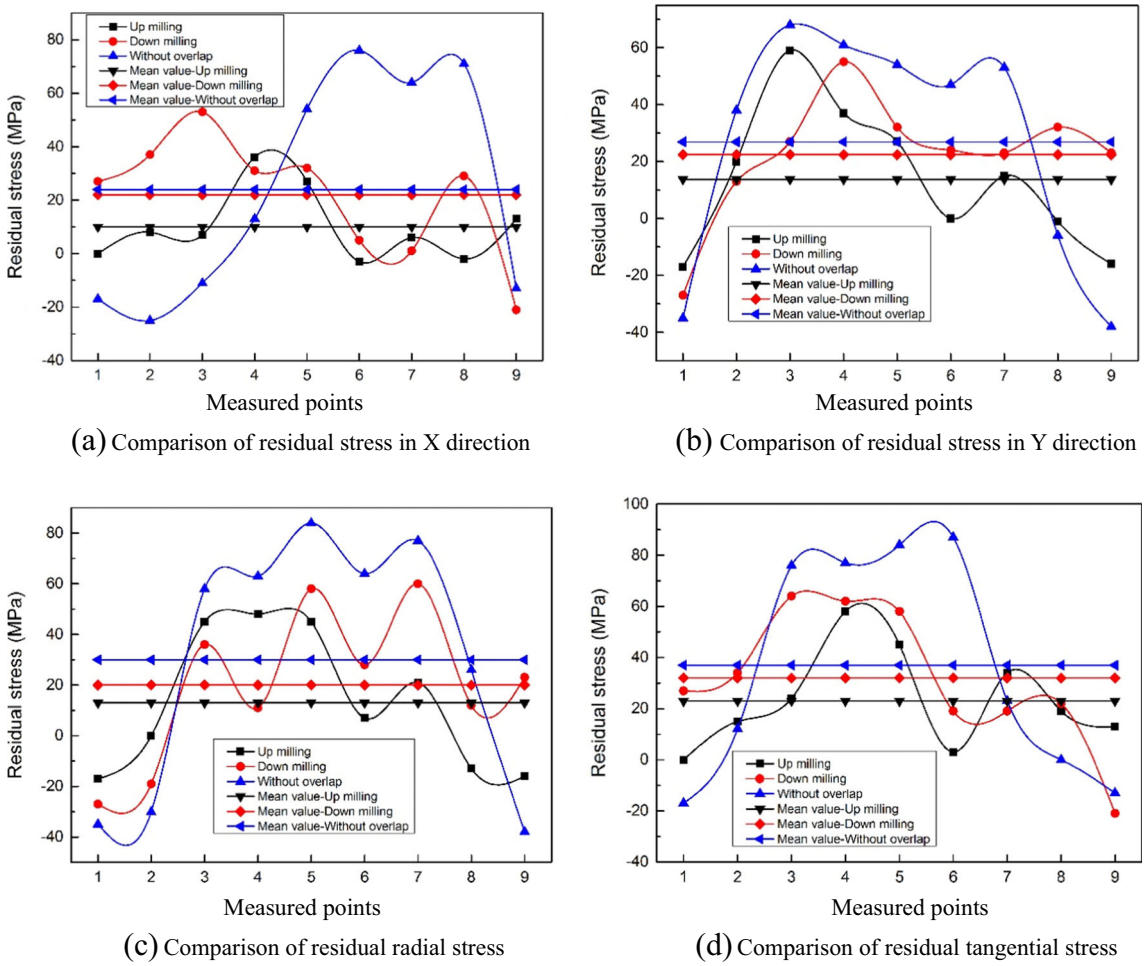

Fig. 9 Effect comparison of redistributed residual stress on the overlap of tool path

Where K is the tool overlap coefficient, D is the tool diameter, and ae is the cutting width.

As shown in the Fig. 11, depending on the position of the different points, the simulation models were established where the tool diameter is 12 mm, the tooth number is 4 and other process parameters are same with Section 2.1. The difference of the superposition region is fully taken into account, with a basis of residual stress analysis model of multiple cuts in Section 2.3. The test rules of points cane be summarized that, the origin point O is the starting point of the width of the workpiece that are divided into four sections with five points (1–5) and the corresponding coordination values being compared and analyzed on the surface residual stress of the different overlapping coefficient (0–1/2). The transverse cutting widths are 12, 10, 9.6, 9, 8, 6 mm, respectively.

As the results shown in Fig. 12, the increase in the overlapping coefficient results in the shrinking value of the workpiece surface residual stress, the reason for which is that in the direction of the transverse cutting width, the amount of material removal falls subsequently, leading to the reduction of the corresponding cutting forces and heat. Since the force and heat are the main factors affecting the generation of the final

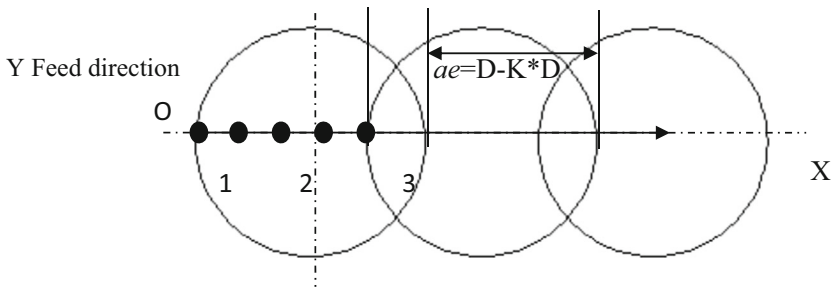

Fig. 10 The definition of tool overlap coefficient in milling process

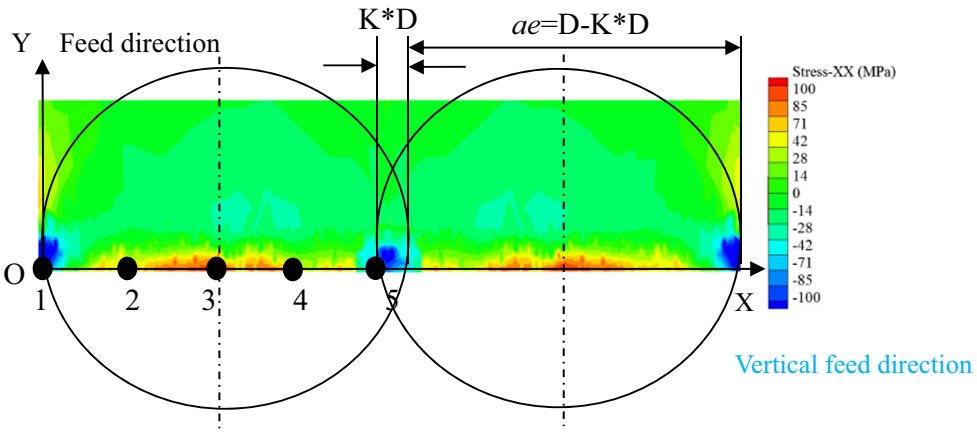

Fig. 11 Sketch of extraction of residual stress after overlapping

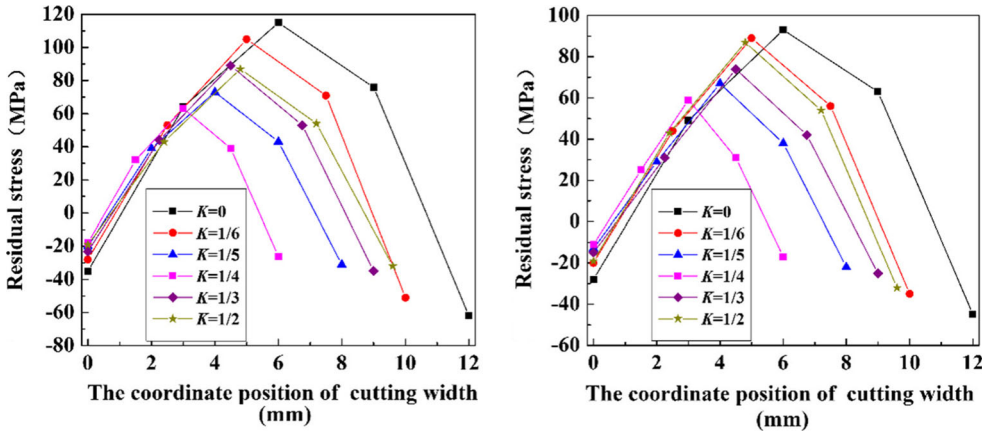

Fig. 12 Effect of overlap coefficient on residual stress of workpiece surface

residual stress, induced residual stress of the workpiece retreats as well. It has been illustrated that the greater the degree of cutting overlap, the smaller the value of residual stress. In other words, the increase or decrease of the overlap coefficient K value is inversely proportional to the growth or shrink of the residual stress value. The results in the figure also suggest that, the maximum residual stress will be obtained in the vicinity of diameter of the tool, and the residual stress around the overlap area becomes smaller. Therefore, in the cutting process of the workpiece, as the overlap area approaching the tool paths, the wave distributions of residual stress will be formed considering residual compressive stress and tensile stress in the workpiece surface, followed by the impact of the different state of tension and compression distribution on the workpiece precision. So, it is of great importance to choose the appropriate *K* value.

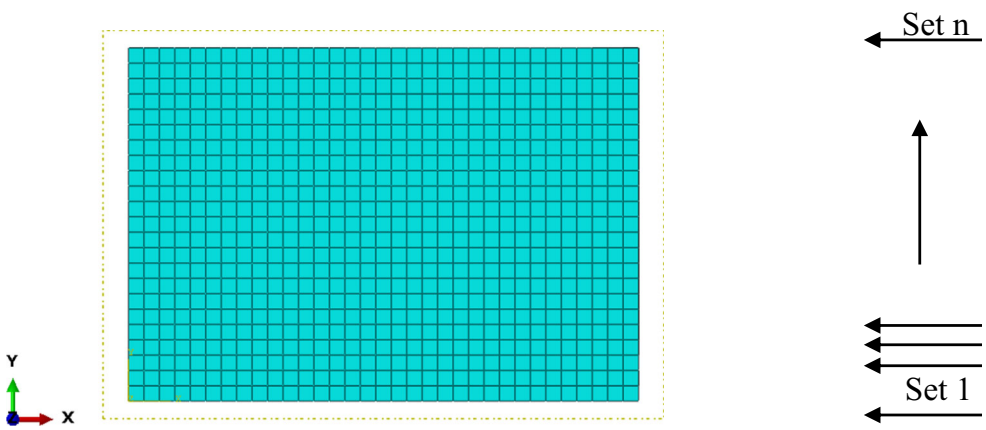

Fig. 13 Mesh generation and sets definition

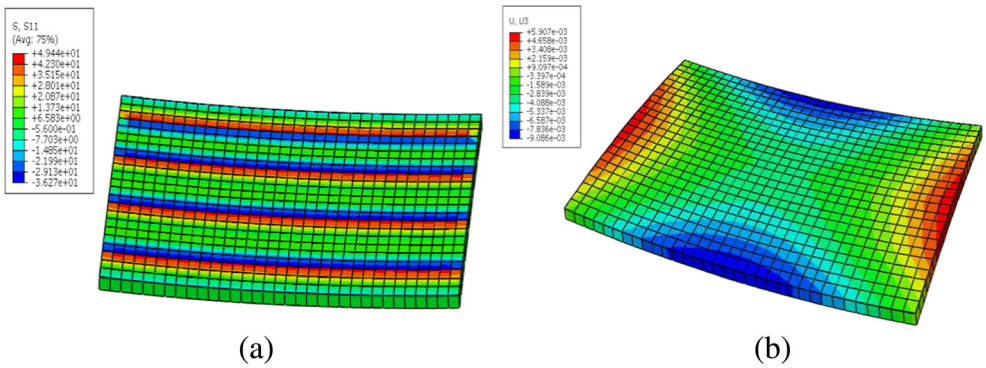

Fig. 14 **a** Residual stress distribution. **b** The influence of residual stress on deformation

3.2 Analysis of the effect of overlap coefficient on the distortion

The redistribution of residual stress noticeably affects the processing deformation of thin-walled parts during or after the machining. Therefore, to discuss the impact of the overlapping coefficient on the deformation of workpiece in this section, six different distributions of residual stress presented in the Fig. 12 are introduced into the finite element software ABQUS (since the minimum thickness of the case part in the Section 3.3 is 2 mm, therefore, the 2 mm thickness of plate workpiece is assumed. Moreover, the length and width are 160 mm and 100 mm respectively). The specific method is elaborated as follows: (1) as presented in the Fig. 13, defining different unit sets along with the tool paths (along the length direction, setting the first unit of part surface as a starting point, the last unit as the end point); (2) According to the name of the set, the profile of residual stress distribution is input as shown in Fig. 12 with the residual stress being defined as a file and the residual stress distribution of the workpiece being demonstrated in the Fig. 14a; (3) The computation work is continued to calculate the distribution of the residual stress on distortion the final workpiece and the distortion contours are given in the Fig. 14b. Here an assumption is added, and uniform residual stresses are used in the analysis, only considering the deflection influence by the residual stress. In the real machining, the more complex distribution of residual stresses is existed.

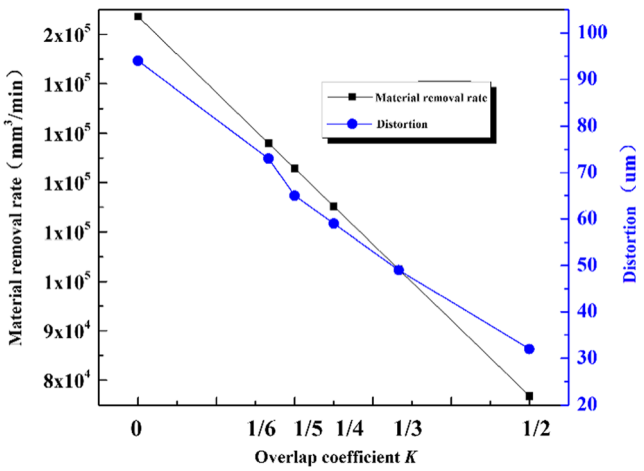

Fig. 15 Effect of overlap coefficient on material removal rate and workpiece deformation

$$Q = Z \cdot f_z \cdot a_p \cdot n \cdot a_e \tag{6}$$

Where Q is the material removal rate (mm^3/min), Z is number of flutes, fz is feed rate (mm/tooth), ap is cutting depth (mm), n is rotational spindle speed (rpm), and ae is radial width of cut (mm).

In this section, the influence of the residual stress of the overlap coefficient from 0~1/2 on the deformation has been fully simulated and analyzed to acquire the maximum deformation value in the Z direction as shown in the Fig. 15. In addition, in order to compare the material removal rate when the other processing parameters are in accordance with the different overlapping regions, according to the Eq.(6), the material removal rate for different combinations of processing parameters is calculated, as shown in the Fig. 15. The finding is clear enough that when the overlap coefficient increases (from 0 to 1/2), the material removal rate is still decreased even though the deformation induced by residual stress is reduced. In the actual machining process, thin-walled part often requires high precision and high efficiency, but these two goals are quite difficult to be achieved together. A better processing efficiency always brings a simultaneous drop in the machining accuracy of the workpiece affected by the residual stress. Similarly, a higher machining accuracy is always accompanied by the reduction in the required material removal rate. Therefore, the overlap coefficient should be careful chosen according to the actual processing.

3.3 Case study for distortion affected by the redistribution of residual stress induced in the end milling of thin-walled part

In order to evaluate the analysis results mentioned above, the aerospace thin-walled part is selected as the study object in this section, and the results of machining residual stress

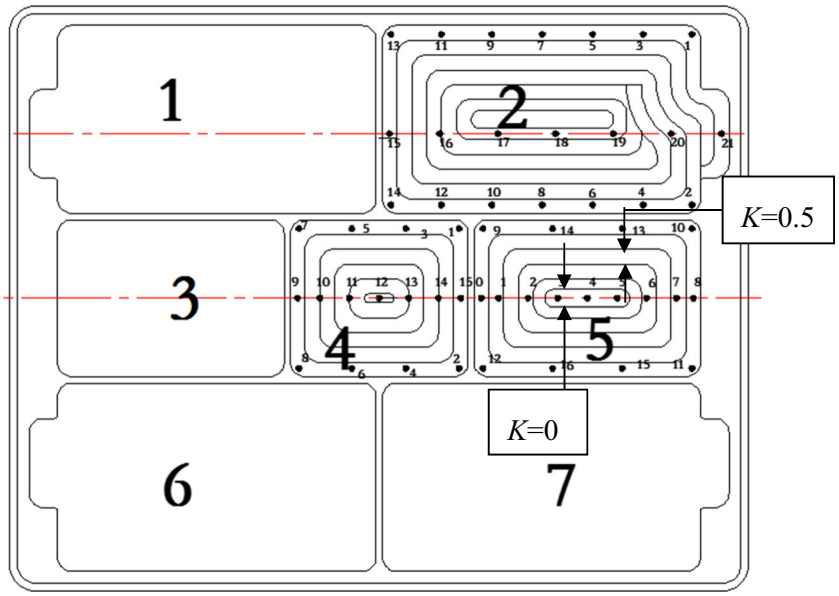

Fig. 16 Measurement scheme of residual stress on the surface of thin-walled parts

distribution and the machining accuracy are obtained and discussed. The case thin-walled part has seven frames, and the wall thickness between each frame is 2 mm, the thickness of the bottom plate is 2 mm, the height is 8 mm, and the width is 249 mm. The aspect ratio of the width and height is 249/8 = 31.125/1, and when the value is 20/1, the utility part is called as thin-walled part. As the conclusions given above, the smaller the K value, the better the machining accuracy achieved. However, during the real production, material removal rate should be also considered. Therefore, in this case study, most area of the part surface is machined with the overlap coefficient 0.5, and the first cut with cutting width is tool diameter (K value is 0).

3.3.1 Residual stress analysis of the thin-walled parts

The residual stress is produced with the new stress in the continuous cutting process, which leads to the redistribution of the residual stress. Due to the consistency of the machining parameters on the top surface and bottom surface of this part, as well as the decreasing rib area on surface, this section is majorly intended for the frame of the part and the residual stress distribution on the bottom surface to test, so that the testing efficiency would be improved with a lower cost. The processing method is demonstrated in the Fig. 3. Since the thin-walled part is characterized with seven frames and the structure is symmetrically distributed, three frames marked by No.2, 4, and 5 are selected to measure and evaluate the residual stress distribution. The measurement plan is shown in Fig. 16, and the results are presented in Fig. 17~Fig. 19.

The surface residual stress distributions of the No. 2, 4, 5 frames are shown in Fig. 17~Fig. 19, and the results revealed the figures well indicate the inconsistency of the distribution of residual stress along different cutting trace. The center of the complete cutting tool path is easy to form residual tensile stress (up to 80 MPa) in the middle region, which allows the

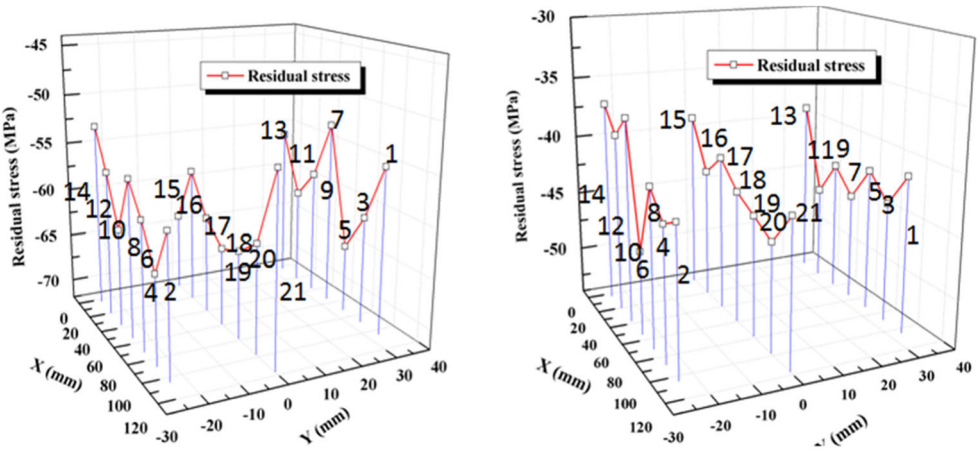

Fig. 17 Residual stress test results of No. 2 box

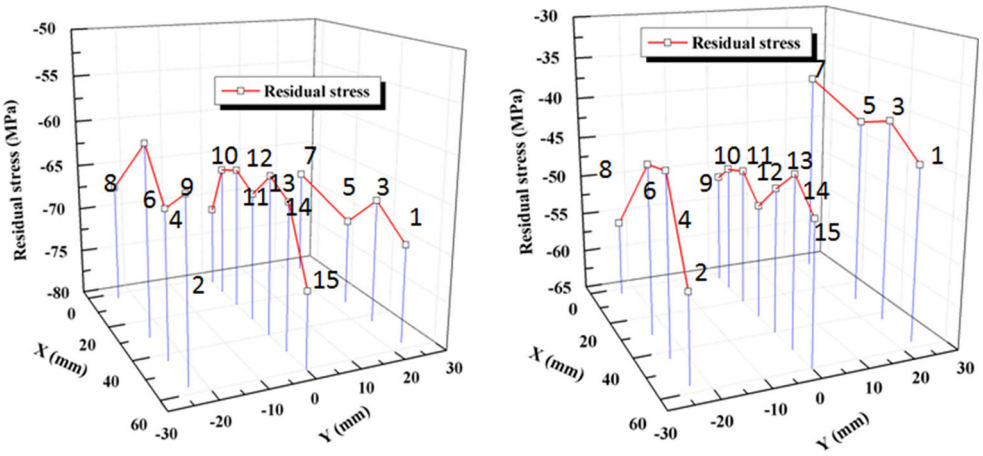

Fig. 18 Residual stress test results of No. 4 box

(a) Vertical feed direction (b) Feed direction

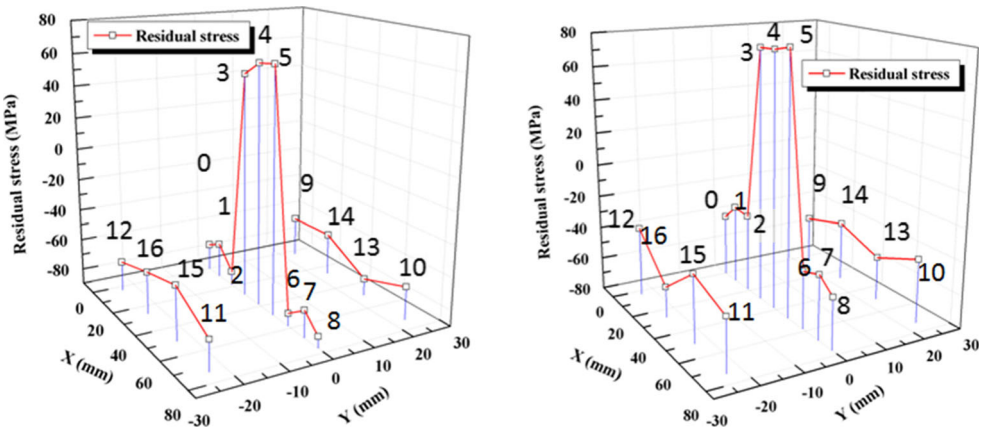

Fig. 19 Residual stress test results of No. 5 box

(a) Vertical feed direction (b) Feed direction

formation of the residual compressive stress (up to −70 MPa) of the tool path superimposed area. According to the distribution of residual stress on the surface of each frame and the milling path, it is known that the distribution of residual stress is varied with different milling paths on the surface of the workpiece during the machining.

As the discussion in the Section 3.1.2, the overlapping coefficient (k) turns smaller leading to the subsequent increase in the deformation caused by the workpiece surface residual stress. It can be also observed from Fig. 16 in this section that, the overlap coefficient in this case study is 0.5 and 0, and according to the test results in Fig. 17, Fig. 18, and Fig. 19, the K value is directly influenced and determined by the overlapping relationship between the tool paths. When the K value gets bigger, the center of the tool path's value gets smaller, such as the points 3, 4, and 5 in Fig. 17 and points 21 and 22 in Fig. 18 and Fig. 19. Another fact is that the final residual stress also goes up when the position of the other test points in the region of the overlap coefficient shrinks. The conclusions are further verified in Section 3.1, where the magnitude of residual stress in the center of the tool path is greater than the distribution in both sides, indicating that in the machining of thin-walled parts with stacking interactions between different tool paths, the material removal rate increases as the overlap coefficient decreases, but accompanied with the increase in the generated residual stress at the same time. Therefore, in order to better control the residual stress distribution, the material removal rate should be appropriately reduced in the

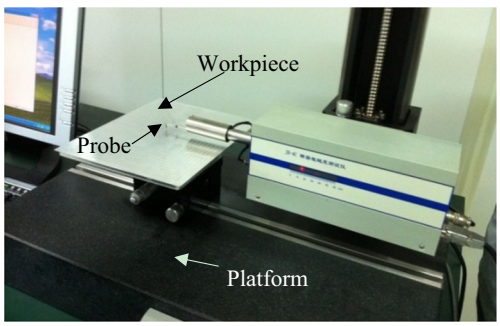

Fig. 20 Roughness measurement of thin wall parts

Table 6 Roughness and flatness of workpiece after roughing and finishing

	Roughness(μm)	Average flatness(mm)
Roughing	0.787	0.089
After heat treatment	0.747	0.085
Finishing—first time	0.238	0.042
Finishing—second time (1 week later)	0.236	0.038
Finishing—third time (1 month later)	0.233	0.044
Finishing—fourth time (6 months later)	0.235	0.043
Finishing—fifth time (1 year later)	0.234	0.042
Finishing—sixth time (2 years later)	0.233	0.041

finishing process, and the overlap coefficient should be raised, so that the subsequent deformation of workpiece caused by the residual stress can be weakened, the machining precision of thin-walled workpiece can be improved, and the production quality can be stably maintained.

In a word, in the milling process of the thin-walled parts, different depths of cutting at different milling stages are all applied according to the requirements of the machining accuracy of thin-walled parts, along with optimizing the selection of overlapping coefficient, so that the cutting force and temperature are controlled to improve the distribution of residual stress on the surface and subsurface of the thin-walled parts, realizing the decrease in the impact of residual stress on the accuracy of thin-walled parts.

3.3.2 Roughness measurement of thin wall parts

After the machining experiments are accomplished, the bottom surface roughness of the thin-walled parts is measured, as shown in the Fig. 20. The measurement results are shown in the Table 6. After the roughing, the depth of cut and the feed rate values have turned to be larger, resulting in that surface roughness value becomes greater than the value after finishing. The thin-walled part roughness is not highly required, eliminating the necessity of much discussion in this section. As the results show, the small surface roughness reduction after 2 years of natural aging may be induced by the temperature variations and measurement error. In a word, the changeable trend of surface roughness is not highly affected by the time.

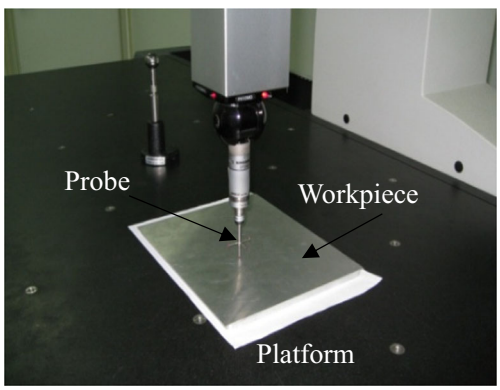

Fig. 21 Deformation measurement of workpiece

3.3.3 Analysis on measurement results of processing deformation

After milling, it is necessary to assess and measure the surface deformation and flatness of the workpiece, with the type of Micro-Hite 3D DCC CMM being adopted to measure the bottom surface flatness of the workpiece after machining, as shown in Fig. 21.

In the machining process of thin-walled parts (the number of test pieces for four pieces), after the completion of the processing, the bottom surface flatness of the workpiece is measured according to the measurement scheme in Fig. 21. The average value of the bottom surface flatness measured in a different period of time (a day, a week, a month, 6 months, 1 year and 2 years) is 0.042 mm (technical requirement from the company is 0.05 mm). Moreover, with the successful control over the deformation, the ultimate maximum deformation of the bottom surface (Fig. 22b) is 0.044 mm, and the measuring error is ±0.003 mm. The maximum deformation of simulation analysis under 4000 rev/min is 0.041 mm (Fig. 22a) in this section. The relative error of experimental and simulated results is 6.82%, possibly originating in the experimental processing machine and test results. Furthermore, certain error also exists in the finite element method. But the results have already proved the correctness of the processing and clamping method at a certain extent, so the effective deformation of the workpiece is validated being reduced by controlling cutting force and thermal and residual stress. Usually, cutting force induces the residual compressive stress, and thermal forms, the residual tensile stress. Moreover, the final residual stress is determined by the comprehensive affections of the force and temperature. The theoretical and experimental bases have been thereby both provided for the control of the machining accuracy of the following parts at the same time.

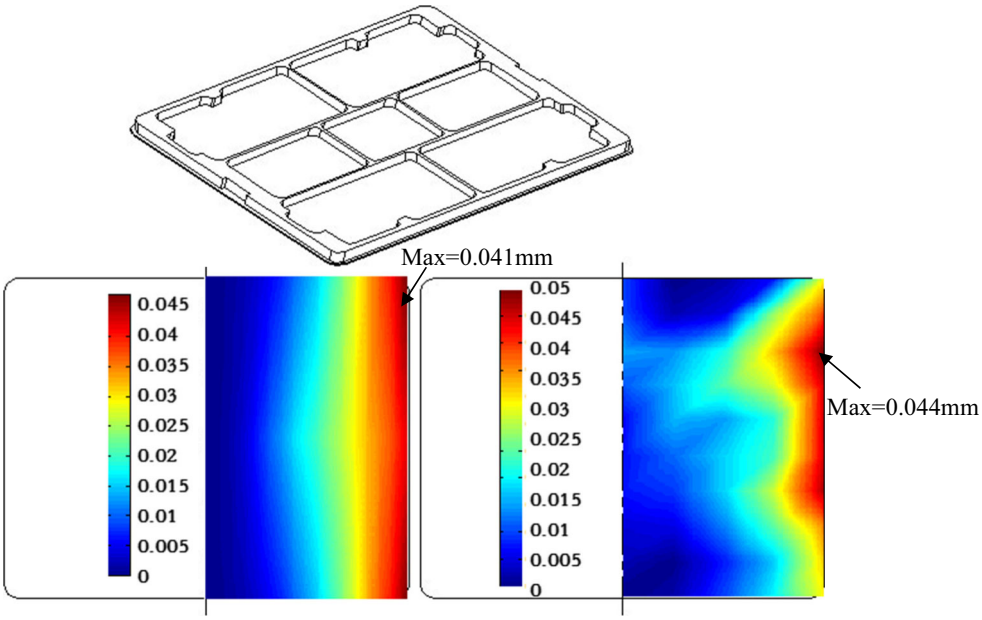

(a) Simulated result (b) Experimental result

Fig. 22 Deformation comparison of simulated and experimental results

4 Conclusions

The tool overlap affections are quite critical to deflection of the thin-walled parts, especially the regenerated residual stress, causing the continuing shape deflection after the machining. FE simulations and experiments are conducted to explore the control approaches. Therefore, combining both theory analysis and experiments, the study has achieved the optimization of redistribution residual stress for the surface and subsurface parts in the multiple processes.

Commonly, the residual stress redistributes in the surface and subsurface of parts during the machining. A model of the overlap coefficient K of the tool path is introduced to analyze the redistribution surface residual stress, supporting the idea that the machined residual stress can be optimized during different processes of roughing and finishing, with optimal combination of the material removal rate and overlap coefficient. Since the Al2024-T3 is selected as the material in the discussion, and different aluminum alloys have the similar variation trend of cutting force and temperature, the conclusions in this study can be adopted to other materials such as 7050-T7451 or 7475-T7351.

Affected by the redistribution of residual stress, the deformation is found to be continuous. The surface residual compressive stress can be formed after the processing is completed, playing a vital role for improving the quality of long-term stability of thin-walled parts.

Through analyzing the influential factors and control methods for the redistribution of residual stress, the summary has been organized that only through reasonable selection and optimization for the residual stress distribution in the multiple processes can it be possible to enhance the stable workpiece quality and improve the shape accuracy.

Acknowledgements This project is supported by National Natural Science Foundation of China (Grant No. 51505291).

References

1. Boiten RG, Cate WT (1952) A routine method for the measurement of residual stresses in plates. Appl Sci Res 3(5):317–343
2. Toshiaki S, Sasahara H, Tsutsumi M (2004) Development of a new tool to generate compressive residual stress within a machined surface. Int J Mach Tools Manuf 44:1215–1221
3. Arunachalam RM, Mannan MA, Spowage AC (2004) Residual stress and surface roughness when facing age hardened Inconel 718 with CBN and ceramic cutting tools. Int J Mach Tools Manuf 44:879–887
4. Navas VG, Gonzalo O, Bengoetxea I (2012) Effect of cutting parameters in the surface residual stresses generated by turning in AISI4340 steel. Int J Mach Tools Manuf 61:48–57
5. Sasahara H, Obikawa T, Shirakashi T (1996) FEM analysis of cutting sequence effect on mechanical characteristics in machined layer. J Mater Process Tech 62:448–453
6. Liu CR, Guo Y (2000) Finite element analysis of the effect of sequential cuts and tool-chip friction on residual stresses in a machined layer. Int J Mech Sci 42:1069–1086
7. Nasr MNA (2015) Effects of sequential cuts on residual stresses when orthogonal cutting steel AISI 1045. Procedia CIRP 31:118–123
8. Wang ZJ, Chen WJ, Zhang YD, Chen ZT, Liu Q (2005) Study on the machining distortion of thin-walled part caused by redistribution of residual stress. Chin J Aeronaut 18(2):175–179
9. Outeiroa JC, Umbrello D, Saoubi RM (2006) Experimental and numerical modelling of the residual stresses induced in orthogonal cutting of AISI 316L steel. Int J Mach Tools Manuf 46:1786–1794

10. Fergani O, Jiang XH, Shao YM, Welo T, Yang JG, Liang SY (2016) Prediction of residual stress regeneration in multi-pass milling. Int J Adv Manuf Technol 83:1153–1160
11. Robinson JS, Tanner DA, Truman CE, Wimpory RC (2011) Measurement and prediction of machining induced redistribution of residual stress in the aluminium alloy 7449. Exp Mech 51:981–993
12. Shao YM, Fergani O, Li BZ, Liang SY (2016) Residual stress modeling in minimum quantity lubrication grinding. Int J Adv Manuf Technol 83:743–751
13. Zeng HH, Yan R, Peng FY, Zhou L, Deng B (2017) An investigation of residual stresses in micro-end-milling considering sequential cuts effect. Int J Adv Manuf Technol. doi:10.1007/s00170-017-0088-5
14. Li JG, Wang SQ (2017) Distortion caused by residual stresses in machining aeronautical aluminum alloy parts—recent advances. Int J Adv Manuf Technol 89:997–1012
15. Treuting RG, Read WT (1951) A mechanical determination of biaxial residual stress in sheet materials. JAppl Phys 22(2):130–134
16. Sosa AD, Echeverria MD, Moncada OJ, Sikora JA (2007) Residual stresses, distortion and surface roughness produced by grinding thin wall ductile iron plates. Int J Mach Tools Manuf 47:229–235
17. Omar F, Lazoglu I, Ali M, Mohamed EM, Liang SY (2014) Analytical modeling of residual stress and the induced deflection of a milled thin plate. Int J Adv Manuf Technol 75:455–463
18. Omar F, Ali M, Lazoglu I, Yang JG, Liang SY (2014) Prediction of residual stress induced distortions in micro-milling of Al7050 thin plate. Appl Mech Mater 472:677–681
19. Sasahara H (2005) The effect on fatigue life of residual stress and surface hardness resulting from different cutting conditions of 0.45%C steel. Int J Mach Tools Manuf 45:131–136
20. Li BZ, Jiang XH, Yang JG, Liang SY (2015) Effects of depth of cut on the distortion and redistribution of residual stress during the milling of thin-walled part. J Mater Pro Technol 216:223–233
21. Jing S, Liu CR (2004) The influence of material models on finite element simulation of machining. J Manuf Sci Eng 126:849–857
22. Bil H, Kılıc SE, Tekkaya AE (2004) A comparison of orthogonal cutting data from experiments with three different finite element models. Int J Mach Tools Manuf 44:933–944
23. Third Wave Systems, I. (2010). AdvantEdge v5.6-014 Machining Simulation Software. Inc Minneapolis, MN.
24. Marusich TD, Ortiz M (1995) Modelling and simulation of high-speed machining. J Num Meth in Eng 38(21):3675–3694
25. T.D. Marusich, E. Askari. (2001). Modeling residual stress and workpiece quality in machined surfaces. Third Wave Systems, Inc Minneapolis.